Mechanisms of artemether toxicity on single cardiomyocytes and protective effect of nanoencapsulation

Ana Carolina Moreira Souza, Andrea Grabe-guimaraes, Jader dos Santos Cruz, Artur Santos-miranda, Charlotte Farah, Liliam Teixeira Oliveira, Alexandre Lucas, Franck Aimond, Pierre Sicard, Vanessa Carla Furtado Mosqueira, et al.

ARTEMETHER TOXICITY MECHANISMS ON SINGLE CARDIOMYOCYTES AND PROTECTIVE EFFECT OF NANOENCAPSULATION

Ana Carolina Moreira Souza, Andrea Grabe-guimaraes, Jader dos Santos Cruz, Artur Santos-miranda, Charlotte Farah, Liliam Teixeira Oliveira, Alexandre Lucas, Franck Aimond, Pierre Sicard, Vanessa Carla Furtado Mosqueira, et al.

Mechanisms of artemether toxicity on single cardiomyocytes and protective effect of nanoencapsulation

Ana Carolina Moreira Souza[1,2] Andrea Grabe-Guimarães[1]
Jader dos Santos Cruz[3] Artur Santos-Miranda[3] Charlotte Farah[2]
Liliam Teixeira Oliveira[1,2] Alexandre Lucas[4] Franck Aimond[2]
Pierre Sicard[2] Vanessa Carla Furtado Mosqueira[1] Sylvain Richard[2]

[1]Pharmaceutical Sciences Graduate Program (CiPharma), Pharmacy School, Federal University of Ouro Preto, Ouro Preto, Minas Gerais, Brazil

[2]Physiologie et Médecine Expérimentale du Cœur et des Muscles (PhyMedExp), Université de Montpellier, CNRS, Inserm, Montpellier, France

[3]Department of Immunology and Biochemistry, Federal University of Minas Gerais, Belo Horizonte, Minas Gerais, Brazil

[4]Institut des Maladies Métaboliques et Cardiovasculaires (I2MC), Inserm/Université Paul Sabatier UMR1048, Toulouse, France

Correspondence
Dr. Sylvain Richard, Physiologie et Médecine Expérimentale du Cœur et des Muscles (PhyMedExp), Inserm U1046, CNRS UMR 9214, Université de Montpellier, CHU Arnaud de Villeneuve, 371, Avenue du Doyen Gaston Giraud, 34295 Montpellier Cedex 05, France.
Email: sylvain.richard@inserm.fr

Funding information
Coordenação de Aperfeiçoamento do Pessoal de Nível Superior; Ministère de l'Europe et des Affaires étrangères; Ministère de l'Enseignement supérieur, de la Recherche et de l'Innovation, Grant/Award Numbers: 13 and Me 978/13, Me 978/20; Conselho Nacional de Desenvolvimento Científico e Tecnológico, Grant/Award Number: 310463/2015-7; National Institute of Science and Technology of Pharmaceutical Nanotechnology, Grant/Award Number: 465687/2014-8; Minas Gerais Research Foundation, Grant/Award Number: APQ-02576-18; NANOBIOMG Network-Minas Gerais, Grant/Award Number: RED-00007-14; FAPEMIG, Grant/Award Numbers: 00432-13, CDS-PPM-00481-13

Background and Purpose: The artemisinin derivative, artemether, has antimalarial activity with potential neurotoxic and cardiotoxic effects. Artemether in nanocapsules (NC-ATM) is more efficient than free artemether for reducing parasitaemia and increasing survival of *Plasmodium berghei*-infected mice. NCs also prevent prolongation of the QT interval of the ECG. Here, we assessed cellular cardiotoxicity of artemether and how this toxicity was prevented by nanoencapsulation.

Experimental Approach: Mice were treated with NC-ATM orally (120 $mg \cdot kg^{-1}$ twice daily) for 4 days. Other mice received free artemether, blank NCs, and vehicle for comparison. We measured single-cell contraction, intracellular Ca^{2+} transient using fluorescent Indo-1AM Ca^{2+} dye, and electrical activity using the patch-clamp technique in freshly isolated left ventricular myocytes. The acute effect of free artemether was also tested on cardiomyocytes of untreated animals.

Key Results: Artemether prolonged action potentials (AP) upon acute exposure (at 0.1, 1, and 10 μM) of cardiomyocytes from untreated mice or after in vivo treatment. This prolongation was unrelated to blockade of K^+ currents, increased Ca^{2+} currents or promotion of a sustained Na^+ current. AP lengthening was abolished by the NCX inhibitor SEA-0400. Artemether promoted irregular Ca^{2+} transients during pacing and spontaneous Ca^{2+} events during resting periods. NC-ATM prevented all effects. Blank NCs had no effects compared with vehicle.

Conclusion and Implications: Artemether induced NCX-dependent AP lengthening (explaining QTc prolongation) and disrupted Ca^{2+} handling, both effects increasing pro-arrhythmogenic risks. NCs prevented these adverse effects, providing a safe alternative to the use of artemether alone, especially to treat malaria.

KEYWORDS
Action potential prolongation, CamKII phosphorylation, enhanced Na^+/Ca^{2+} exchange, pro-arrhythmogenic risks, spontaneous Ca^{2+} waves

Abbreviations: ACT, artemisinin-based combination therapies; AP, action potential; DLS, dynamic light scattering technique; EADs, early afterdepolarizations; LV, left ventricular; NCs, nanocapsules; NCX, membrane-bound Na^+/Ca^{2+} exchanger; PCL, poly-ε-caprolactone; PDI, polydispersity index; PLB, phospholamban; SERCA, sarco/endoplasmic reticulum Ca^{2+}-ATPase; SL, sarcomere length; SR, sarcoplasmic reticulum; VA, ventricular arrhythmia; WHO, World Health Organization.

1 | INTRODUCTION

Malaria is a mosquito-borne infectious disease caused by protozoa of genus *Plasmodium* sp., which represents a major health problem. According to the World Health Organization (WHO), malaria is endemic in nearly 100 countries and territories, particularly in underprivileged areas of Africa, Asia, and Latin America. In 2018, there were 228 million cases of malaria and an estimated 405,000 malaria deaths (WHO, 2018). In absence of an effective malaria vaccine, chemotherapy is still an unavoidable strategy to fight the disease. Unfortunately, the resistance of *Plasmodium falciparum* to several antimalarial drugs, such as chloroquine and mefloquine, is increasing dramatically (Lehane, McDevitt, Kirk, & Fidock, 2012; Price et al., 2004). Combinations of drugs are the most successful strategy used in malaria chemotherapy (Oguche et al., 2014; Sowunmi et al., 2017) Artemether–lumefantrine, artesunate–amodiaquine, dihydroartemisinin–piperaquine, artesunate–mefloquine, and artesunate–sulfadoxine–pyrimethamine are first-line treatment protocols used in countries where malaria is endemic -(WHO, 2018). They rely mainly on the use of artemisinin derivatives such as **artemether**, a semisynthetic sesquiterpene lactone.Despite antimalarial effectiveness on schizonticide and gametocide activities (Brossi et al., 1988), **artemether** presents several drawbacks including a short half-life, cardiotoxicity, neurotoxicity, haematological toxicity and immunotoxicity (Gu, Cui, Wu, Shi, & Teng, 1989; Silamut et al., 2003; Yin et al., 2014). Regarding cardiotoxicity, several experimental studies have shown that rat and dog treatment with **artemether** (Yin et al., 2014), artesunato (Yin et al., 2014), or arteether by intramuscular or oral route prolongs the QT interval of the ECG. We have recently shown that oral administration of **artemether** at doses of 40, 80, and 120 $mg{\cdot}kg^{-1}$ caused QT and QTc interval prolongation on both uninfected and *Plasmodium berghei*-infected mice (Souza et al., 2018). QT interval prolongation is an electrocardiographic surrogate marker of drug toxicity. It predisposes to torsades de pointes and is frequently associated with occurrence of malignant ventricular arrhythmia (VA), potentially leading to sudden death (Chan, Isbister, Kirkpatrick, & Dufful, 2007; Isbister & Page, 2013). Different cellular mechanisms can be involved in drug-induced QT interval prolongation, including blocking of outward I_{Kr} and I_{Ks} currents; alteration in Ca^{2+} cycling; and activation of persistent inward I_{Na} current (Haverkamp, Breithardt, Camm, & Janse, 2000). It is therefore important to perform in vitro studies to identify the molecular effects of **artemether**, understand any potential cardiotoxicity and find alternatives to reduce those effects.

Polymeric nanocapsules (NCs) have been developed to reduce adverse effects and toxicity of different drugs (Branquinho, Roy, et al., 2017; Leite et al., 2007; Mosqueira et al., 2004). NCs are nanocarriers with an oily core in which lipophilic drugs are transported (Legrand, Barratt, Mosqueira, Fessi, & Devissaguet, 1999). NCs are able to modify drug release profile by altering biodistribution and bioavailability (Branquinho, Roy, et al., 2017). Recently, we demonstrated the potential of NCs to reduce cardiotoxic effects of oral administration of free **artemether** at doses of 40, 80, and 120 $mg{\cdot}kg^{-1}$ in both uninfected and *P. berghei*-infected mice. In addition, NCs containing **artemether** (NC-ATM) were effective in combating malaria, achieving both cure and increasing the survival rate of mice by oral route (Souza et al., 2018). Given that, it was necessary to understand the effect of free **artemether** on cardiomyocytes. We focused on the excitation–contraction coupling of single cardiomyocytes from mice, and we investigated the mechanisms involved. Additionally, we tested whether the use of NCs is a valuable strategy for preventing potential adverse effects after in vivo repeated-dose treatment of mice, in conditions similar to those of clinical therapy.

What is already known

- Artemether is a standard drug to treat uncomplicated and severe malaria, even in children.
- Nanoencapsulation maintains artemether effectiveness against *Plasmodium berghei* while reducing its cardiotoxicity in vivo.

What this study adds

- Free artemether induced action potential lengthening, due to Na^{+}–Ca^{2+} overactivity, and disturbed Ca^{2+} handling.
- Orally administered nanocapsules-artemether prevents cellular cardiac alterations induced by free-artemether and the associated pro-arrhythmogenic risks.

What is the clinical significance

- The encapsulation of artemether in polymeric nanocapsules is a potential approach to treat severe malaria.
- It could also be applied to therapeutic approaches against other parasites and tumours.

2 | METHODS

2.1 | NCs preparation and artemether in vitro release kinetics

We prepared PCL blank-NCs, or loaded with **artemether**(NC-ATM), by the polymer deposition method followed by solvent displacement as described before (Fessi, Puisieux, Devissaguet, Ammoury, & Benita, 1989). Polymer (PCL, 24 mg), soy lecithin (Epikuron ™ 170, 30 mg), and 100 μl of **artemether** oil solution (80 $mg{\cdot}ml^{-1}$) were dissolved briefly in 2.0 ml of acetone. The aqueous phase was prepared with complete dissolution of 30 mg of poloxamer 188 in 8 ml of MilliQ water. Organic phase was then poured into aqueous

phase using a syringe; the mixture was maintained under agitation for 10 min; and solvents were evaporated under reduced pressure (Heildolph Rotary Evaporator Instruments, Germany) until reaching 2-ml final volume with 4 mg·ml^{-1} of artemether in colloidal suspension of NCs. Blank-NCs were prepared as described above in the absence of artemether and using 100 μl of Miglyol 812 as the NCs oily core. The mean hydrodynamic diameter, polydispersity index (PDI), and ζ potential of NCs were determined using Zetasizer NanoZS equipment (Malvern Instruments, UK), dynamic light scattering technique (DLS), and DLS coupled with microelectrophoresis for size and ζ potential measurements, respectively. NC-ATM were developed previously and characterized in detail by our group, and more than 90% of artemether was encapsulated in NCs (Vidal-Diniz, 2014). Free artemether was prepared as suspension mixing 0.09 g of artemether with 0.3 g of carboxymethylcellulose and 2.0 ml of sorbitol dispersed in 15 ml of MilliQ water. Vehicle (control solution) was prepared similarly, but in the absence of artemether. We maintained the formulations at controlled temperature, protected from light, and we prepared them freshly on the day of treatment.

In vitro studies of dissolution kinetics of free artemether and release kinetics of artemether from NCs were conducted using the inverted dialysis method in PBS (pH 7.4) under sink conditions (20% of saturation solubility) previously determined as 14 μg·ml^{-1} at 37°C. Free form artemether crystals (1.4 mg) or 350 μl of ATM-PCL NCs (concentration of 4 mg·ml^{-1}) were placed at time 0 in 500 ml of PBS release media at 37°C in a thermostatic shaker bath containing five dialysis sacks (SpectraPor 12,000–14,000 MWCO) with 1 ml of PBS. At each time interval (0, 5, 30, 60, and 120 min), a dialysis sack was withdrawn simultaneously with a sample of release media (500 μl). The samples were diluted 1:1 with acetonitrile, then vortex-mixed, centrifuged at 500×*g* for 5 min, and supernatant assayed by HPLC-UV to determine artemether concentrations using a validated method (da Cesar & Pianetti, 2009). Three independent experiments were conducted, with each one tested in triplicate.

2.2 | Animals

All animal care and experimental procedures conformed to Directive 2010/63/EU of the European Parliament and the Council of September 22, 2010, for animal protection. Animal studies are reported in compliance with the ARRIVE guidelines (Kilkenny, Browne, Cuthill, Emerson, & Altman, 2010) and with the recommendations made by the British Journal of Pharmacology. The project was approved by the French Ministère de la Recherche et de l'Enseignement Supérieur (N° 02571.01) and the local institutional animal research committee (Languedoc Roussillon, CEEA-LR-1069). The experiments also complied with the guidelines established by the Brazilian College of Animal Experimentation (COBEA).

Here, we used 6- to 8-week-old male C57BL/6J mice weighing 20–22 g (Janvier Labs, Saint Berthevin, France) for all experiments. Animals were bred and housed (four to five mice in each cage) under pathogen-free conditions in a temperature-regulated room (22 ± 2°C; 12-h day/12-h night cycle) and an environment to meet their physical needs (standard rodent chow diet and ad libitum access to water) and behavioural needs (wood bedding material, cardboard tunnel, nesting material, and wooden gnawing sticks). The animals were killed humanely by cervical dislocation according to Directive 2010/63/EU of the European Parliament and of the Council of September 22, 2010, on the Protection of Animals Used for Scientific Purposes. This method allows rapid death without injection of any substance that might interfere with cell electrophysiology for cell studies. In order to reduce the number of animals (3Rs), we made efforts to use cells isolated from one animal for different protocols performed in parallel (e.g., patch-clamp, different recording conditions, and Ca^{2+} fluorescence imaging).

Mouse models of malaria using P. berghei are well established, usable and cost-effective for studying different aspects of human infections including parasite–host interaction, antimalarial treatments, drug resistance, T cell mediated immunity, antigenic variation, and erythrocyte invasion pathways (Burgert et al., 2020; Hernandez-Valladares, Rihet, & Iraqi, 2014; Kurup, Butler, & Harty, 2019; Patel, Simpson, Batty, & Zaloumis, 2015). Here, we tested only male mice in order to follow up our previous studies showing the efficacy of NC-ATM in P. berghei-infected male mice (Souza et al., 2018). We sought to compromise between a reasonable number of animals (Sneddon, Halsey, & Bury, 2017) used and the results necessary to answer our main questions (artemether toxicity and protective effect of nanoencapsulation).

2.3 | In vivo treatment protocol

We first studied the acute cellular effects of artemether in vitro following the application of 0.1, 1.0, and 10 μM of the free artemether on single cardiomyocytes obtained from untreated animals (n = 16) and tested in different experimental conditions. Effects in the artemether group were compared to the control group exposed to DMSO:Tween (as the vehicle to artemether used acutely) diluted appropriately in the buffer medium to obtain the same in vitro concentrations. For repeated-dose treatments, the mice were blindly randomized to the four different groups: vehicle (n = 10), blank-NCs (n = 11), free-ATM (n = 11), and NC-ATM (n = 10 mice). Unrelated animals were randomized individually to cages, then cages were randomized to treatment groups housed in the same environment (same shelves) before starting the protocol. We administered treatments by oral route at 120 mg·kg^{-1}, twice daily (12/12 h) for 4 days (eight oral administrations). Treatment administration was not blinded to avoid complexity and errors due to the handling of animals. We could use only two animals (from two different groups) per day for single-cell recordings (Ca^{2+} imaging and cellular electrophysiology) requiring prior enzymic isolation of the cardiomyocytes. The start of the protocol was therefore shifted sequentially for each "pair" of animals in order to meet this requirement. The animals were treated identically with administrations by the same experimenter and at the same

times of the day throughout the experiment. Animals were assigned randomly to Ionoptix, patch-clamp experiments, biochemistry, and echocardiography.

2.4 | Single cardiomyocyte isolation

Cardiomyocytes were isolated from mice with no treatment and from mice treated with **artemether** formulations (free form or NCs) or with control solutions (vehicle or blank-NCs). The cell isolation procedure was initiated 2 h after administration of the last dose (day 4, eigth dose). The heart was perfused by means of the Langendorff system for enzymic treatment and the use of 0.1 $g \cdot ml^{-1}$ liberase (high research grade; Roche, Basel, Switzerland) circulated at a flow rate of 5–10 $ml \cdot min^{-1}$ for 6–8 min at 37°C as described before (Branquinho, Roy, et al., 2017).

2.5 | Sarcomere contraction and measurements of intracellular Ca^{2+}

Sarcomere length (SL) shortening, an index of contraction, and intracellular Ca^{2+} transients of left ventricular (LV) myocytes loaded with fluorescent ratiometric Ca^{2+} indicator Indo-1AM (2 mM, Invitrogen Grand Island, NY, USA) were monitored with an IonOptix system (Milton, MA, USA) as described before (Branquinho, Roy, et al., 2017). Cells were field-stimulated with 1-ms current pulses delivered via two platinum electrodes at 1.0 Hz and illuminated at 365 nm by means of a Xenon arc bulb light. Cytosolic Ca^{2+} was determined by Indo-1AM fluorescence, which emits at 405 and 480nm concurrently (ratio of 405 nm/480 nm). To assess occurrence of abnormal macroscopic Ca^{2+} events, cells were stimulated for a period of 30 s, followed by rest period of 30 s.

2.6 | Cellular electrophysiological recordings

Whole-cell voltage- and current-clamp experiments (HEKA, Harvard Bioscience, Inc., Holliston, MA, USA) were performed (22–24°C) on freshly isolated LV cells. For action potential (AP) measurements, a 1-nA pulse lasting 2–4 ms was applied, at a frequency of 1 Hz for 5 min. Pipette solution was filled with (in mM) 20 KCl; 10 HEPES; 130 KOH; 130 aspartic acid; 2 $MgCl_2$; and 5 NaCl (pH 7.4). The cell bath solution contained (in mM) NaCl 130; KCl 4; $MgCl_2$ 1.8; $CaCl_2$ 1.8; HEPES 10; and glucose 11 (pH 7.4). To evaluate the acute effects of free **artemether** (10 μM) on the AP waveform, freshly isolated myocytes were incubated for 15 min before recording. To assess the contribution of the **Na^+/Ca^{2+} exchanger (NCX)** and the late Na^+ current ($I_{Na,Late}$) in the effect of **artemether** on AP, cells were exposed to 1-μM **SEA-0400** or 20-μM **ranolazine**, respectively, in presence of **artemether**. Currents were digitally sampled at 10 kHz, and their amplitude was normalized to whole-cell membrane capacitance (current densities $pA \cdot pF^{-1}$). In all whole-cell experiments, cells were kept at rest for 2 min prior to any experimental protocol in order to allow proper equilibration between cell media and intracellular pipette solution. Moreover, cells with total series resistance over 8 MΩ were not considered in the analysis to prevent voltage-clamp errors.

2.7 | Biochemistry and western blot analysis

For biochemistry, perfused isolated hearts from mice were acutely exposed to **artemether** (10 μM) for 15 min using the Langendorff technique. Simple Western (Jess, ProteinSimple, CA) was based on capillary electrophoresis (CE) and offers a size assay that combines CE-SDS with immunodetection to separate proteins by MW (Schiattarella et al., 2019). The separated proteins were attached to the capillary wall by a proprietary photo-activated chemical crosslink. Subsequent immunodetection was achieved automatically by incubating and washing the capillary with primary and secondary antibodies conjugated with HRP and detected via chemiluminescence. Protein expression was measured by peak area with Compass software (Bio-Techne, ProteinSimple). Diluted protein lysate was mixed briefly with fluorescent master mix and heated at 37°C for 10 min. Protein mix (3 μl), total protein normalization reagent, blocking reagent, wash buffer, target primary antibody, secondary HRP (ready to use DM-001 "detection module"), and chemiluminescent substrate were dispensed into designated wells in a manufacturer-provided 66–440 kDa of matrix microplate (SMW 004, ProteinSimple). We used Anti-phospholamban antibody (ab85146; Abcam, France), phospho-Ser^{16}-PLB and phospho-Thr^{17}-PLB (Badrilla, A010-12 and A010-13, respectively; UK), and home-made phospho-Ser^{2808}-RyR2 and phospho-Ser^{2814}-RyR2 antibodies. The Immuno-related procedures used comply with the recommendations made by the *British Journal of Pharmacology*.

2.8 | Data and statistical analysis

The data and statistical analysis comply with the recommendations of the *British Journal of Pharmacology* on experimental design and analysis in pharmacology (Curtis et al., 2018).

For in vitro studies, cells were chosen randomly. Data analyses were performed blinded for experimenters as much as possible. Reported values are means ± SEM, except for **artemether** in vitro kinetic study (mean ± SD). D'Agostino and Pearson omnibus and Shapiro–Wilk normality tests were used. Comparisons between groups of more than two samples were made using one-way ANOVA. Where ANOVA was used, post hoc tests were conducted only where F was significant ($P < 0.05$) and there was no variance inhomogeneity. Tukey post-test was used to compare all pairs of columns using GraphPad Prism software version 6.0 (GraphPad Software Inc., San Diego, CA, USA). Unpaired two-sample t tests were used when appropriate. Only those studies where each group size was at least five animals were analysed statistically and are indicated by symbols in the graphs. N indicates the number of mice, and n indicates the number of independent cardiomyocytes isolated from these mice. Differences

were considered significant when $P < 0.05$. Data on the number of arrhythmic cells were analysed using Fisher's exact test. $P < 0.05$ was determined as significant. The data that support the findings of this study are available from the corresponding author upon reasonable request.

2.1 | Materials

We purchased artemether (dihydroartemisinin methyl ether), poly-ε-caprolactone (PCL), poloxamer 188 (Pluronic®F68), carboxymethylcellulose, and HPLC grade acetone from Sigma-Aldrich (Sigma-Aldrich Co., St. Louis, MO, USA). The solution of artemether dissolved in oil was produced by the National Malaria Control Program, Ministry of Health, Brazil. Soy lecithin with approximately 75% of phosphatidylcholine (Epikuron™ 170) was a generous gift from Cargill (Germany). We purchased Miglyol®812N from Sasol Germany GmbH. MilliQ water was purified using a Symplicity® System (Millipore, Bedford, USA). We protected free artemether and NC-ATM from direct light exposure throughout the experiments.

2.2 | Nomenclature of targets and ligands

Key protein targets and ligands in this article are hyperlinked to corresponding entries in the IUPHAR/BPS Guide to PHARMACOLOGY (http://www.guidetopharmacology.org) and are permanently archived in the Concise Guide to PHARMACOLOGY 2019/20 (Alexander, Fabbro et al., 2019; Alexander, Kelly et al., 2019; Alexander, Mathie, et al., 2019).

3 | RESULTS

3.1 | NCs preparation and release kinetics of artemether in vitro

The NC-ATM formulations used in the present work have been characterized previously (Souza et al., 2018). The blank NCs and ATM-NCs were monodispersed formulations (PDI < 0.3) of colloidal particles that presented mean hydrodynamic sizes of 197 and 254 nm, and negative ζ potential of −56 and −50 mV, respectively, which account for their colloidal stability due to electric repulsion between particles. The polymeric NCs were able to encapsulate artemether in high concentrations (4 mg·ml^{-1}), which could be due to the high lipophilicity of artemether (log P_{ow} 3.53). NCs maintain their colloidal stability and artemether content under storage for at least 3 months at 4°C (Souza et al., 2018). in vitro release of artemether from the NCs device was evaluated. Results showed low artemether release after incubation for 30 min (∼15%) and 2 h (∼45%) compared to faster dissolution of free artemether (∼32% and ∼95%, respectively) (Figure 1). NCs acts as a device to prolong artemether release, and direct comparison of free artemether and ATM-NCs may be influenced by the difference in release kinetics. We thus used the free drug to identify the major mechanisms of artemether toxicity on cardiomyocytes.

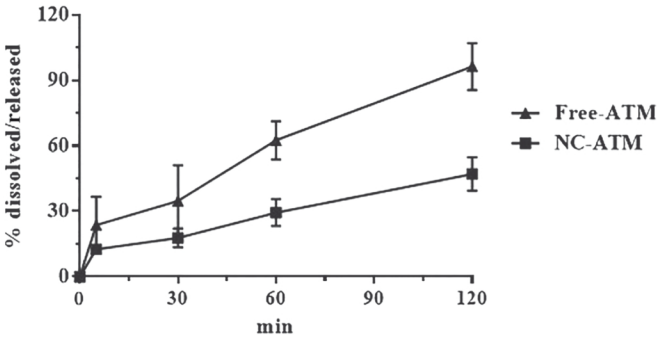

FIGURE 1 The release of artemether from NCs is slower than the dissolution of the free form of artemether. Dissolution/release profiles of artemether as free compound (free artemether; ATM) and as loaded in polymeric nanocapsules (ATM-NC) in phosphate buffer saline at 37°C in *sink* conditions. Data shown are means ± SDs of $n = 3$ independent experiments. The assay was made in triplicate (nine measures in total) to ensure the reliability of single values

3.2 | Acute in vitro effect of artemether on cell contraction and Ca^{2+} cycling

We examined the cellular and molecular effects of 0.1-, 1.0-, and 10-μM free artemether on SL shortening and intracellular Ca^{2+} of LV cardiomyocytes freshly isolated from control animals and investigated within 1 to 4 h after cell isolation. The acute effects of artemether are illustrated in Figure 2a,b. Artemether had no significant effects on SL shortening, or on either the amplitude or decay of the Ca^{2+} transient (Figure 2c,d,f). However, free artemether, at all concentrations, caused a reduction in diastolic Ca^{2+} (Figure 2e). Free artemether also promoted irregular Ca^{2+} transients during pacing and abnormal spontaneous Ca^{2+} waves during resting periods, which were not seen in untreated cells or cells exposed to vehicle (Figure 3a–e). The number of cells exhibiting these aberrant Ca^{2+} events increased dose-dependently with maximal effects seen at 1 and 10 μM (Figure 3f).

3.3 | Acute post-translational effects of artemether on phospholamban and ryanodine receptors

As we did not expect changes of protein expression during acute effects of artemether, we explored post-translational modifications of proteins involved in altered Ca^{2+} handling (Figure 4). Cardiac sarco-endoplasmic reticulum Ca^{2+}-ATPase (SERCA2a) activity ensures the uptake of Ca^{2+} in the sarcoplasmic reticulum (SR) during the relaxation and diastolic period. SERCA2a activity is critically regulated by the inhibitory protein phospholamban (PLB) in various physiopathological situations (Minamisawa et al., 1999). phosphorylation at Serine16 (Ser^{16}-PLB) by cAMP-dependent protein kinase (PKA), or Threonine17 (Thr^{17}-PLB) by calmodulin-dependent protein kinase II

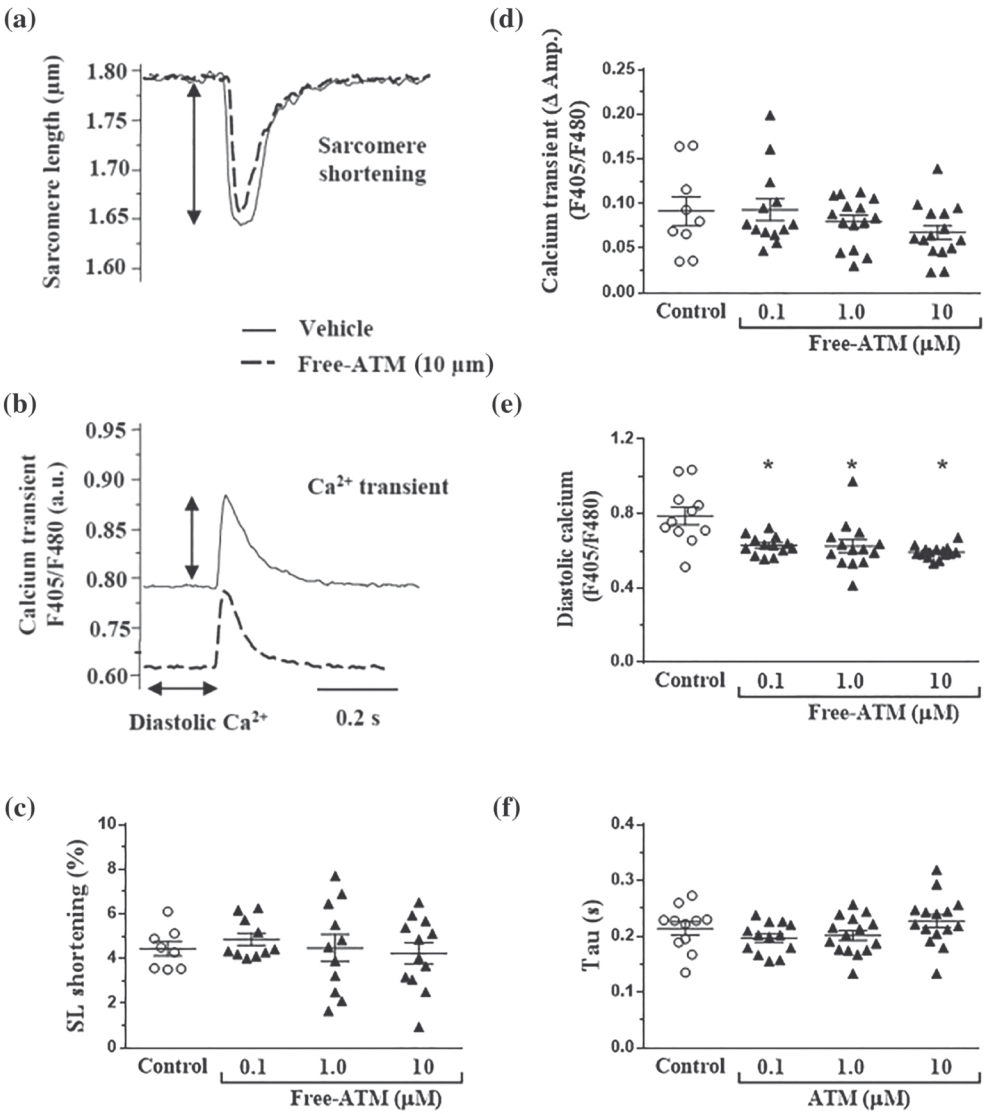

FIGURE 2 Acute effect of free artemether on sarcomere length (SL) shortening and Ca^{2+} transient in left ventricular myocytes isolated from untreated mice. Freshly isolated cells were exposed to free artemether (ATM) for 15 min at concentrations of 0.1 μM (n = 13, N = 5), 1.0 μM (n = 15, N = 5), and 10 μM (n = 15, N = 5), or to vehicle (control; n = 9, N = 5). Contraction and Ca^{2+} transients were evoked by electrical pacing at 1.0 Hz. (a, b) Typical records of the effect of ATM (10 μM) or vehicle on sarcomere length (SL) shortening (a) and Ca^{2+} transient (b). (c–f) Averaged effects of ATM (at 0.1, 1.0, and 10 μM) on SL shortening (c), Ca^{2+} transient (d), Ca^{2+} diastolic (e), and Ca^{2+} transient decay (Tau) (f). Data shown are means ± SEM; n values as indicated above. $^{*}P < 0.05$, significantly different from control at all concentrations; one-way ANOVA followed by Tukey's post hoc test

(CaMKII), relieves this inhibition and enhances the rate of Ca^{2+} uptake (Hagemann & Xiao, 2002). Acute application of free artemether (10 μM) promoted phosphorylation at the CaMKII-specific Thr^{17}-PLB site but not at the PKA-specific Ser^{16}-PLB (Figure 4a–c). Post-translational modifications of the cardiac ryanodine receptor RyR2 protein, which controls SR Ca^{2+} release during excitation–contraction coupling, are also identified as one of the molecular mechanisms responsible for Ca^{2+} handling alterations (Denniss, Dulhunty, & Beard, 2018; Niggli et al., 2013). Free artemether promoted RyR2 phosphorylation at Serine(S)2814 but not at S2808 (Figure 4d–g).

3.4 | Acute effect of artemether on cardiomyocyte AP

Myocyte contraction and intracellular Ca^{2+} dynamics are conditioned by cell excitability. Typical APs of LV myocytes isolated from untreated animals were recorded (Figure 5a). Free artemether acutely applied in vitro markedly prolonged the AP (Figure 5a, bottom panels; Figure 5b,d). We investigated the potential involvement of the repolarizing voltage-gated outward K^+ currents in this effect. The different components, namely, $I_{to,f}$ (fast component of the transient outward current), $I_{K,slow}$ (slow inactivating outward K^+ current), and I_{ss} (sustained outward K^+ current), in AP repolarization were recorded as described in the Supporting Information. Free artemether had no effect on the global K^+ current (Figure S1). Detailed analysis confirmed that the drug affected neither the $I_{to,f}$ (responsible for the early AP repolarization) nor $I_{K,slow}$ (slow inactivating outward K^+ current) involved in late AP repolarization (Figure S1).

Any increase in an inward current could also account for the marked delayed repolarization of the AP. The $I_{Na,Late}$ current was a good candidate to test. We used ranolazine, a selective inhibitor of $I_{Na,Late}$ reported to be 38-fold more potent in inhibiting $I_{Na,Late}$ than peak (transient) I_{Na} (Belardinelli, Shryock, & Fraser, 2006; Undrovinas, Belardinelli, Undrovinas, & Sabbah, 2006). Figure 5a (left panel) shows that ranolazine (20 μM) had no effect on the AP, both in control conditions and after application of artemether (10 μM). Therefore, the results showed that ranolazine did not prevent the effect of artemether on AP repolarization (Figure 5a, left panel; Figure 5b,c), suggesting that promotion of $I_{Na,Late}$ by artemether does not contribute to the effect of artemether on AP duration.

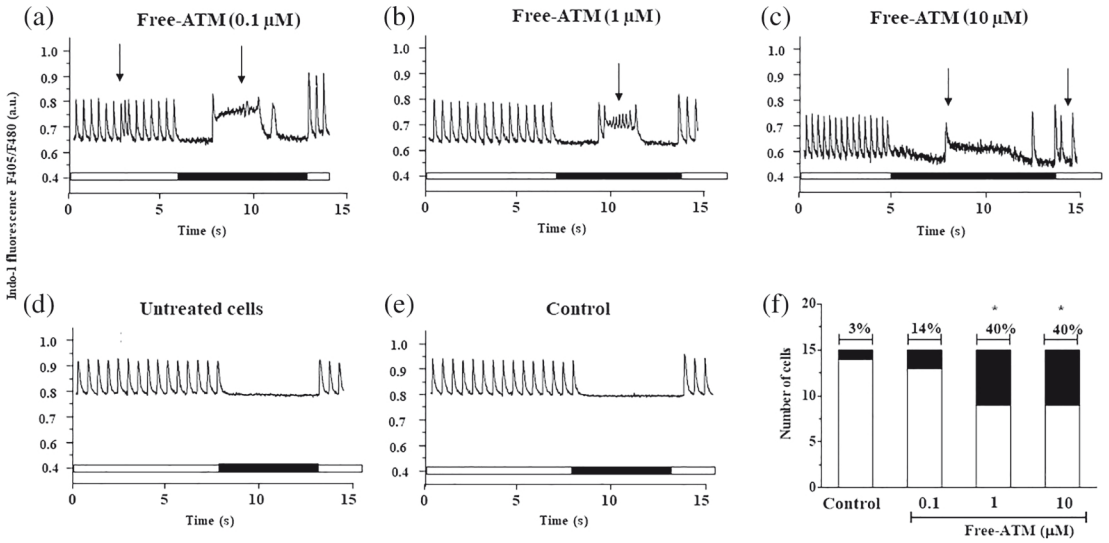

FIGURE 3 Acute exposure to free **artemether** promotes irregular Ca^{2+} transients during pacing and spontaneous diastolic Ca^{2+} events in left ventricular myocytes, isolated from untreated mice. Freshly isolated cells (n = 15 isolated from N = 5 mice in each group) were exposed to free **artemether** (Free-ATM) for 15 min at concentrations of 0.1 (a), 1.0 (b), and 10 μM (c) or to vehicle (control). Ca^{2+} transients were evoked by electrical pacing at 1.0 Hz (horizontal bars, white colour), followed by a resting period (horizontal bars, black colour) (a–e). ATM promoted aberrant Ca^{2+} events (indicated by arrows) at all concentrations tested during pacing and resting periods. (f) Summary data. Number of cells exhibiting abnormal Ca^{2+} events at 0.1-, 1.0-, and 10-μM Free-ATM versus control (e) and untreated cells (d). Data shown are means ± SEM; n values as indicated above. $^{*}P < 0.05$, significantly different from control; Fisher's exact test

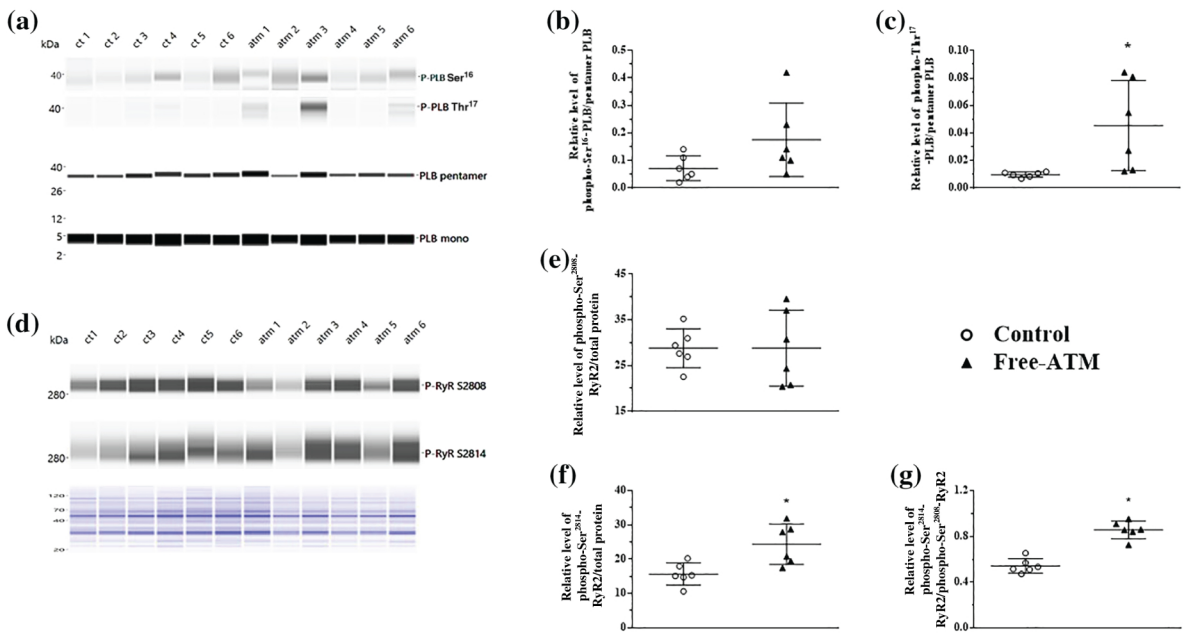

FIGURE 4 Activation of CaMKII-dependent phosphorylation of PLB and RyR2 after acute exposure of isolated hearts to **artemether**. Isolated hearts were exposed acutely to **artemether** (Free ATM; 10 μM; n = 6 mice) or vehicle (control; N = 6 mice) for 15 min using the Langendorff perfusion technique. Representative western blots of the effects of **artemether** on (a) PLB phosphorylation at Serine16 (Ser^{16}-PLB) by cAMP-dependent protein kinase (PKA) and Threonine17 (Thr^{17}-PLB) by calmodulin-dependent protein kinase II (CaMKII), and (b) phosphorylation of RyR2 at Serine-(S)2814 by CaMKII, and at Serine-(S)2808 as possible phosphorylation sites for PKA. (c) Relative level of phospho-Ser^{16}-PLB/pentamer PLB. (d) Relative level of phospho-Thr^{17}-PLB/pentamer PLB. (e) Relative level of phospho-Ser^{2808}RyR2/total protein. (f) Relative level of phospho-Ser^{2814}RyR2/total protein. (g) Relative level of phospho-Ser^{2814}RyR2/phospho-Ser^{2808}RyR2. In panels (c)–(g), data shown are means ± SEM; $^{*}P < 0.05$, significantly different from control; unpaired t test

To explore further the mechanism involved in the effect of ATM, we investigated the role of the membrane bound NCX. The NCX is a bidirectional regulator of cytosolic Ca^{2+} that plays a key role in Ca^{2+} homeostasis during excitation–contraction coupling of cardiomyocytes (Shattock et al., 2015). The NCX is particularly essential for removing intracellular Ca^{2+} during relaxation. The NCX

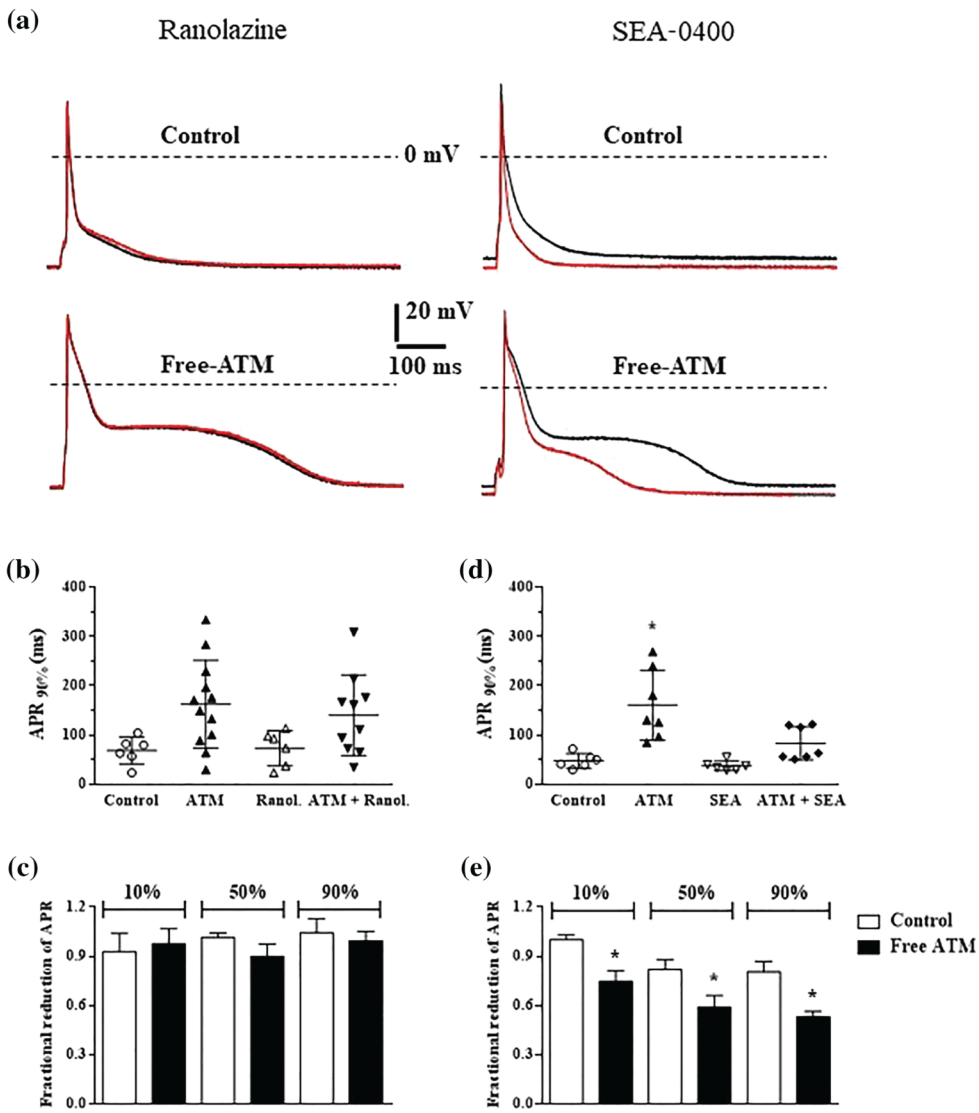

FIGURE 5 The prolongation of AP by free artemether is antagonized by SEA-0400 but not by ranolazine. (a) Representative AP records from isolated LV myocytes exposed for 15 min with vehicle (control; upper panels) or free artemether (ATM, 10 μM; lower panels). Black lines are control APs, while red lines are APs after exposure to 20-μM ranolazine (left panels) or 1-μM SEA-0400 (right panels) in the presence of free artemether; panel (b) presents summarized data of the time required to reach 90% of AP repolarization after exposure to ranolazine (Ranol; $n = 6$, $N = 5$) compared to control ($n = 6$, $N = 5$), ATM ($n = 12$, $N = 5$), and ATM + Ranol ($n = 10$, $N = 5$); panel (d) presents summarized data of the time required to reach 90% of AP repolarization after exposure to SEA-0400 (SEA; $n = 6$, $N = 5$) compared to control ($n = 6$, $N = 5$), ATM ($n = 7$, $N = 5$), and ATM + SEA ($n = 7$, $N = 5$). Fractional reduction of AP repolarization (APR) time starting at AP maximal amplitude after exposure to ranolazine (c) and SEA-0400 (e) in the presence of ATM was plotted at 10%, 50%, and 90% of repolarization. In panels (b)–(e), data shown are means ± SEM; n values as indicated above. $^{*}P < 0.05$, significantly different from control; one-way ANOVA followed by Tukey's post hoc test

forward mode enables Ca^{2+} removal and generates a depolarizing inward Na^{+} current that can be pro-arrhythmogenic. SEA-0400 selectively inhibits both forward and reverse modes of the NCX (Ozdemir et al., 2008; Tanaka et al., 2002). SEA-0400 is expected to reduce Ca^{2+} overload due to the reverse mode and reduce NCX-related Na^{+} entry (against Ca^{2+} extrusion) in the forward mode. Results showed that SEA-0400 (1 μM) prevented the lengthening effect of free artemether on AP duration (Figure 5a, right panel; Figure 5d,e). We also noted an intrinsic influence of SEA-0400 on AP duration and a hyperpolarizing action on the resting membrane potential (which is not voltage-clamped) in control. This may have been because the intrapipette solution used was free of Ca^{2+} buffer EGTA, thereby enabling access to compartmentalized signals including Na^{+}/Ca^{2+} modulation of the NCX. Overall, this observation is consistent with a role of NCX current in controlling cardiomyocyte resting membrane potential.

3.5 | Effects of repeated doses of artemether and NC-ATM administered in vivo on cell contraction and Ca^{2+} cycling

We investigated the effects of repeated-dose treatment administered to mice of free artemether (120 $mg \cdot kg^{-1}$) on parameters of the

excitation–contraction coupling in paced single intact LV myocytes. We measured SL shortening (cell contraction) and intracellular Ca^{2+}. Free artemether decreased cell contraction (Figure 6a,c) and Ca^{2+} transient amplitude (Figure 6b,d) but had no effect on Ca^{2+} transient decay (Figure 6e). Diastolic Ca^{2+} was decreased (Figure 6b,e). Irregular Ca^{2+} transients during pacing and spontaneous Ca^{2+} waves during resting periods occurred (Figure 7a,e). We did not observe these effects in other experimental conditions (Figure 7b–e). To summarize, any of the effects associated with free artemether treatment on contraction and Ca^{2+} handling were observed in the control groups (vehicle and blank-NCs). Importantly, encapsulation of artemether (NC-ATM) prevented the effects of the free form of the drug (Figures 6 and 7).

3.6 | Effects of repeated dose of free artemether and NC-ATM administered in vivo on cardiomyocyte AP and L-type calcium current

We investigated the effect of free artemether treatment on cellular electrical activity and Ca^{2+} entry, two major determinants of the Ca^{2+} transient and associated cellular contraction. Figure 8a shows typical AP recorded in all experimental conditions. Treatment with free-artemether markedly delayed AP repolarization (Figure 8a). Indeed, APD_{90} was increased but not APD_{50} (Figure 8b,c). In contrast, no effect was observed in the control groups (vehicle and blank-NCs). The prolonging effect of free artemether on AP duration was fully prevented by its nanoencapsulation (NC-ATM). The other parameters such as resting membrane potential (Figure 8d), AP amplitude (Figure 8e), and the maximum rate of depolarization (dV/dt_{max}) were not changed significantly.

The contraction of cardiac cells is largely determined by the rise of intracellular Ca^{2+} initiated by the transmembrane Ca^{2+} entry carried out by inward L-type Ca^{2+} current ($I_{Ca,L}$). Repeated treatment of mice with free artemether, as well as with vehicle, blank-NCs, or NC-ATM, had no effect on the $I_{Ca,L}$ waveform (Figure S2A). There was no change in the peak current amplitude (reported as density) or decay kinetics. Evaluation of the current-to-voltage relationship (Figure S2B), steady-state activation (Figure S2C), and voltage-dependent availability for activation (Figure S2D) also showed no difference. Therefore, the reduction of the Ca^{2+} transient was neither related to a decrease nor a prolongation of AP duration related to a modification in the amplitude or properties of $I_{Ca,L}$.

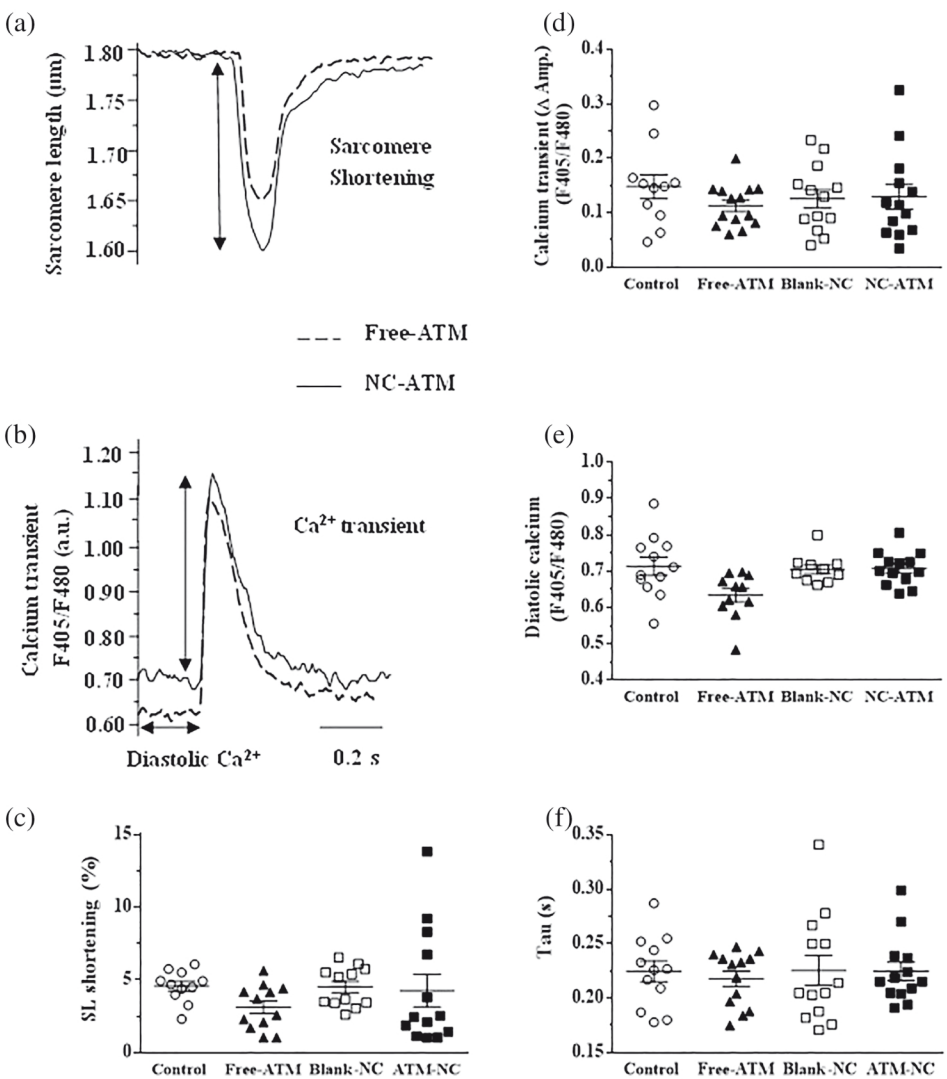

FIGURE 6 Nanoencapsulation prevents the effects of repeated-dose treatment of mice with artemether on the contraction and the Ca^{2+} transient in freshly isolated single LV myocytes. Mice were treated with vehicle (control), free artemether (Free-ATM, 120 $mg \cdot kg^{-1}$), blank-NCs, or NC-ATM (120 $mg \cdot kg^{-1}$). (a, b) Representative contraction and Ca^{2+} transient evoked by electrical field stimulation at 1.0 Hz in single myocytes from the ATM and NC-ATM groups after 4 days of treatment; (a) contraction as measured from sarcomere length (SL) shortening; (b) Ca^{2+} transient expressed as the fluorescence ratio F405/F480. (c–f) Averaged effects in single myocytes isolated from the control (n = 12, N = 4), ATM (n = 11, N = 4), blank-NCs (n = 13, N = 4), and NC-ATM groups (n = 13, N = 4); (c) SL shortening (%); (d) Ca^{2+} transient; (e) diastolic Ca^{2+}; and (f) Ca^{2+} transient decay (Tau). In panels (c)–(f), data shown are means ± SEM; n values as indicated above

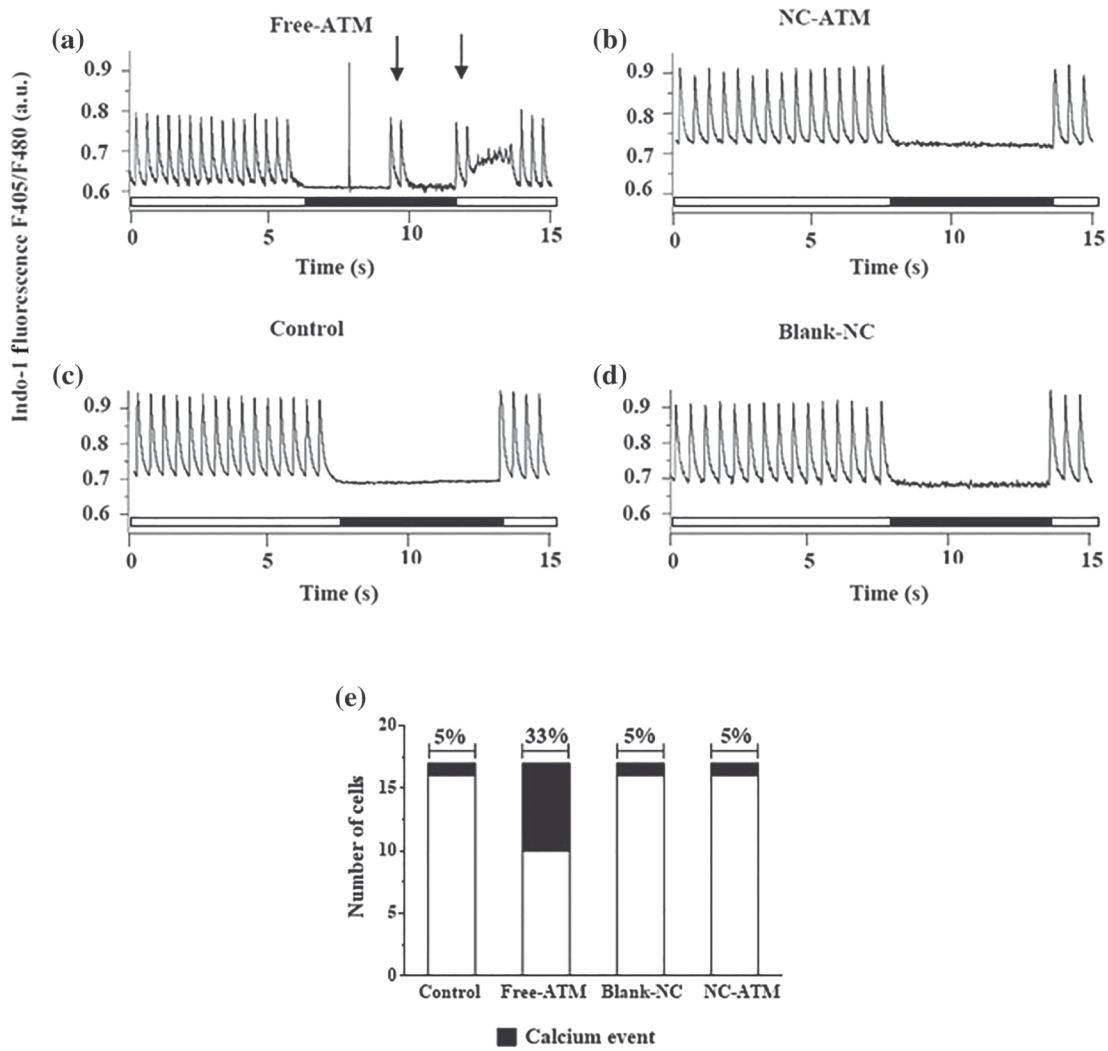

FIGURE 7 Nanoencapsulation prevents the occurrence of irregular Ca^{2+} transients during pacing and spontaneous diastolic Ca^{2+} events in single left ventricular myocytes following repeated-dose treatment of mice with artemether. Mice were treated with vehicle (control), free artemether (Free-ATM; 120 mg·kg^{-1}), blank-NCs, or NC-ATM (120 mg·kg^{-1}). Ca^{2+} transients were evoked by electrical pacing at 1.0 Hz (horizontal bars, white colour), followed by a resting period (horizontal bars, black colour). (a) artemether promoted aberrant spontaneous Ca^{2+} events (indicated by arrows) during pacing and resting periods, which was prevented by nanoencapsulation (b) and not seen with vehicle (c) or blank-NCs (d). (e) Number of cells exhibiting abnormal Ca^{2+} events in the control (n = 17, N = 4), free-ATM (n = 17, N = 4), blank-NCs (n = 17, N = 4), and NC-ATM (n = 17, N = 4) groups. Data shown are means ± SEM; N values as indicated above

3.7 | Effects of repeated dose of artemether and NC-ATM administered in vivo on heart morphology and function

Because cardiomyocyte contraction was decreased, we examined heart morphology and function by echocardiography at the end of the 4-day repeated-dose treatments (Figure S3). When compared to the control group (vehicle), free artemether had no effect on the diameter of the LV lumen (Figure S3A), measured as the LV internal diameter (LVID) in diastole, or the thickness of both the LV anterior wall (AW) and the LV posterior wall (PW) (Figure S3B,C). Functional parameters such heart rate (HR) and the ejection fraction (EF) reflecting systolic function were not modified (Figure S3D,E). The E/A ratio, reflecting the early passive (E-wave) and late atrial contraction (A-wave) components of LV filling, was also unchanged (Figure S3F). No parameters were affected by artemether administered in its encapsulated form (NC-ATM group; Figure S3). Altogether, these results showed that the 4-day repeated-dose treatment with artemether induced neither morphological nor functional changes in line with an absence of cardiac remodelling.

4 | DISCUSSION

Artemether is an effective drug for reducing parasitaemia in malaria and increasing the survival of mice infected with *P. berghei* (Souza et al., 2018). Remarkably, effectiveness of artemether and other antimalarial drugs can be improved by nanoencapsulation that prolongs their effect (Haas, Bettoni, de Oliveira, Guterres, & Dalla Costa, 2009; Leite et al., 2007; Mosqueira et al., 2004; Souza et al., 2018).

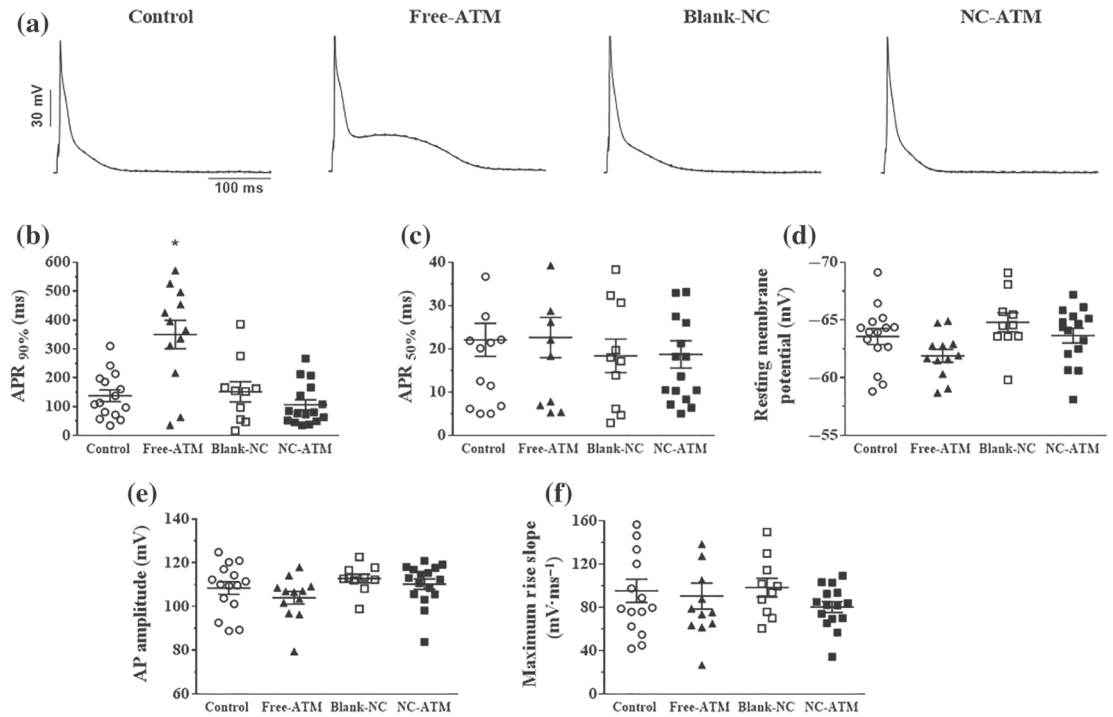

FIGURE 8 Nanoencapsulation prevents the effect of artemether on the action potential in single left ventricular myocytes following repeated-dose treatment of mice with ATM. (a) Representative AP of LV myocytes isolated from mice treated with vehicle (control; n = 15, N = 4), free-ATM (n = 9–12, N = 4), blank-NCs (n = 10, N = 4), or NC-ATM (120 mg·kg^{-1}; n = 16, N = 4); (b, c) time required to reach, respectively, 90% and 50% of AP repolarization (APR); (d) mean resting membrane potential of cardiomyocytes; (e) mean AP amplitude; and (f) maximum rate of AP depolarization. In panels (b)–(f), data shown are means ± SEM; n values as indicated above

However, a legitimate question is whether higher efficacy induces artemether toxicity, as suggested by QT and QTc interval prolongation in mice, and whether nanoencapsulation can prevent adverse cellular effects. Our present results have shown that free artemether modifies cellular electromechanical coupling and induces pro-arrhythmogenic effects. Our data also provided evidence that the nanoencapsulation of artemether prevented its adverse cardiac effects.

The cardiotoxicity risk of antimalarial drugs has received much attention. These drugs can affect myocardial depolarization and repolarization. For example, primaquine, quinine and quinidine block inward Na^+ current, which depresses the maximal upstroke velocity of the AP (Grace & Camm, 1998; Orta-Salazar, Bouchard, Morales-Salgado, & Salinas-Stefanon, 2002). Risks of VA have also been identified from QTc interval prolongation due to delayed repolarization (Yin et al., 2014). Chloroquine, halofantrine, lumefantrine, and mefloquine have reported molecular effects including the blockade of L-type Ca^{2+} currents and K^+ currents, such as I_{Kr} and I_{Ks}, involved in the AP plateau and repolarization (White, 2007). Anti-cholinergic action of artemisinin on $I_{K,ACh}$ may also occur via inhibition of the muscarinic K^+ channel and/or associated GTP-binding proteins (Hara et al., 2007).

Here, we report critical cellular effects of repeated oral administration of artemether (120 mg·kg^{-1}; twice daily, 12/12 h) for 4 days in mice. The in vivo treatment reproduced the effects of acute myocyte exposure to free artemether on AP duration and abnormal Ca^{2+} events. Overall, these results are in line with a direct and rapid effect of the drug (de Vries & Dien, 1996). This also excluded the possibility that the effects seen after repeated administration in vivo result from cardiac remodelling, unlikely to occur within the 4-day treatment (Svoboda, Poprach, Dobes, Kiss, & Vyzula, 2012), which was confirmed by our investigation of heart morphology and function by echocardiography. Incidentally, the reduction of myocyte contraction after treatment with free artemether was not found on myocardial function, either because this effect is modest (or not significant upon acute exposure of single cells) or because the negative inotropy is compensated by one or more mechanisms external to the cell, such as neurohormonal system(s).

One major result of our study was that NCX overactivity accounts for the artemether-induced lengthening of AP duration (Figure 5). The delay in AP repolarization occurs at potentials less than −50 mV; that is, when the fast repolarizing K^+ current I_{to} is mostly inactivated. Free artemether consistently had no effect on I_{to}. Although attenuation of $I_{K,slow}$ can prolong late AP repolarization and the QT interval (Xu et al., 1999), we discarded this possibility. Likewise, we also discounted any effect of artemether on $I_{Ca,L}$ (on both amplitude and decay kinetics), as well as a promotion of the $I_{Na,Late}$ current, as ranolazine failed to inhibit the effect of artemether. On the other hand, the NCX inhibitor SEA-0400 successfully abolished AP lengthening (Figure 5), supporting the idea that artemether increases the activity of the NCX operating in forward mode, that is, extruding one Ca^{2+} ion out, in exchange for the entry of three Na^+ ions into the cell (Venetucci, Trafford, O'Neill, & Eisner, 2007). This mechanism is also

consistent with lowered diastolic intracellular Ca^{2+} (Figures 2 and 6). Our results are in line with a previous report showing that SEA-0400 shortens AP duration and increases diastolic $[Ca^{2+}]_i$ (Bourgonje et al., 2013).

QTc prolongation, a surrogate marker of VA risks, provides a substrate for early afterdepolarizations (EADs). Our study demonstrated the involvement of NCX in the QTc prolongation induced by **artemether** (Souza et al., 2018). As women have longer QT_c and a greater intrinsic sensitivity to QT prolonging drugs than men (Darpo et al., 2014), extrapolation of the NCX-dependent AP and QTc (Souza et al., 2018) prolongations in mice may suggest a critical drug-induced delay in cardiac repolarization reserve in women. This aspect warrants further investigation in a more appropriate experimental model (Salama & Bett, 2014). Our results disclosed another type of risk due to occurrence of abnormal spontaneous intracellular Ca^{2+} events during diastole (Figures 5 and 8) that can trigger Ca^{2+}-dependent VA (Pasquié & Richard, 2009). Increased Na^+ entry through NCX may generate sufficient depolarization for ectopic activation of voltage-gated Na^+ channels and the triggering of abnormal APs and Ca^{2+} transients during diastole. In addition to NCX, **artemether** also boosted the activity of a set of Ca^{2+} handling proteins involved in excitation–contraction coupling, but also in arrhythmias in case of imbalance due to pathological situations. In normal conditions, Ca^{2+} removal from the cytosol by the SERCA2a pump, responsible for intracellular Ca^{2+} uptake and storage in the cardiac SR, prevails over NCX activity. PLB phosphorylation enhances the SR Ca^{2+} load through enhanced SERCA2a activity, whereas RyR2 phosphorylation produces the opposite effect by promoting SR Ca^{2+} leak (Denniss et al., 2018; Hagemann & Xiao, 2002; Niggli et al., 2013). Our results showed that **artemether** induces complex effects known to favour, on one hand, an increased activity of SERCA2a (via PLB phosphorylation) and NCX, and on the other hand, Ca^{2+} leak from the SR via RyR2. As the decline in Ca^{2+} transients was unchanged, a balance may have been established between the different factors. Finally, enhanced extrusion of Ca^{2+} through NCX may explain the decrease in the Ca^{2+} transient and cell contraction because less Ca^{2+} would be available for SR Ca^{2+} uptake (Schillinger, Fiolet, Schlotthauer, & Hasenfuss, 2003).

Artemether rapidly phosphorylated the CaMKII-specific Thr^{17}-PLB site, but not the PKA-specific Ser^{16}-PLB, following acute exposure to the drug. Similarly, free **artemether** promoted phosphorylation of the cardiac ryanodine receptor, RyR2, at Ser^{2814} (but not that at Ser^{2808}). CaMKII-dependent phosphorylation has been associated with pathological RyR2 conformational change that induces abnormal SR Ca^{2+} leak (Uchinoumi et al., 2016). Incidentally, CaMKII activity is increased in the heart under stress or pathological conditions where oxidation is elevated (Anderson, 2015). Remarkably, **artemether** has an endoperoxide bridge, the opening of which by iron leads to the production of free radicals, causing oxidative stress in the parasite (Cumming, Ploypradith, & Posner, 1997). **Artemether** has multiple cellular targets through the involvement of ROS (Kavishe, Koenderink, & Alifrangis, 2017) such as ion channels and transporters that are often implicated in VA (Niggli et al., 2013; Wagner, Rokita, Anderson, & Maier, 2013). RyR2 contains several redox-sensitive cysteine residues and is highly sensitive to ROS, which promotes aberrant SR Ca^{2+} release (Terentyev et al., 2008). Redox-mediated SR Ca^{2+} depletion was proposed to involve reciprocal regulation of SERCA and NCX via direct oxidative modification of both proteins (Kuster et al., 2010). The NCX also has reactive thiols and can be activated by ROS (Goldhaber, 1996; Reeves, Bailey, & Hale, 1986), which could account for the **artemether**-induced increase of NCX activity. Moreover, exposure to modest oxidative stress causes a contractile phenotype characterized by reduced contraction, reduced Ca^{2+} transient, and no effect on diastolic Ca^{2+} (Kuster et al., 2010), relatively similar to modifications induced by **artemether**. Therefore, **artemether**-induced ROS production may disturb, directly or indirectly, a set of Ca^{2+} handling proteins critically involved in VA. Taken together, the pro-arrhythmogenic effects of **artemether** are clearly multifactorial and resemble many effects of ROS. These aspects and the determination of the primary **artemether** targets will require further investigation.

Artemisinin-based combination therapies (ACTs) are recommended for uncomplicated malaria (Plewes, Leopold, Kingston, & Dondorp, 2019; WHO, 2018). **Artemether** is given as first-line oral treatment in combination with lumefantrine to treat malaria due to *P. falciparum* (Belew et al., 2019) and *Plasmodium vivax* (Abreha et al., 2018). As a medical emergency, severe malaria requires rapid parenteral administration. Unfortunately, cardiotoxicity is a major concern with reports of significant prolongation of the QTc interval of ECG in healthy volunteers treated with ACTs (Falade et al., 2008; Funck-Brentano et al., 2019). In an experimental model, **artemether** induced high mortality (50%) and electrocardiographic disorders in mice surviving the parasitaemia (Souza et al., 2018). To circumvent this problem, **artemether** nanocarriers have been developed, including lipid nanoparticles (Aditya, Patankar, Madhusudhan, Murthy, & Souto, 2010), liposomes (Chimanuka, Gabriëls, Detaevernier, & Plaizier-Vercammen, 2002), nanocrystals (Shah et al., 2016), and nanoemulsions (Laxmi, Bhardwaj, Mehta, & Mehta, 2015). Oral drug delivery is a convenient administration route for patients (Attili-Qadri et al., 2013). NC-ATM administered orally not only improved the efficacy of **artemether** against the *Plasmodium* but also prevented QTc prolongation in mice (Souza et al., 2018). Here, we provide additional evidence for the protective effects of NCs against adverse effects of **artemether** shown at the cellular and molecular levels (AP prolongation and Ca^{2+} handling modifications). The lymphatic pathway is involved in the absorption of NCs, protecting **docetaxel** from degradation either in the intestine or systemic circulation, thereby leading to higher blood levels than those achieved with the free drug injected intravenously (Attili-Qadri et al., 2013). A similar mechanism may account for the safer profile of NC-ATM. Another possibility may relate to modified drug distribution and bioavailability, with NCs acting as a reservoir enabling a slow, sustained, release of lower doses of free **artemether** in the circulation, rather than a large but short peak of concentration with free **artemether**, as for halofantrine and lychnopholide (Branquinho, Pound-Lana, et al., 2017; Branquinho, Roy, et al., 2017; Leite et al., 2007). Such a system would be expected to provide more continuous drug coverage for the duration of treatment and therefore increase the effectiveness of therapy.

This may also result in more limited exposure of the heart to the free drug. This advantage has a genuine pharmaceutical potential, as the underlying principle may be extended to other organs and to various parasitic diseases, including toxoplasmosis (Sordet, Aumjaud, Fessi, & Derouin, 1998), Chagas disease (De Mello et al., 2016), leishmaniasis (Chaurasia et al., 2015), and malaria (Mosqueira et al., 2004; Souza et al., 2018). It is worth noting that the therapeutic potential of **artemether** goes far beyond the framework of malaria, as this drug also shows promise for to treating leishmaniasis (Mortazavi Dehkordi, Ghaffarifar, Mohammad Hassan, & Esavand Heydari, 2013), schistosomiasis (El-Beshbishi et al., 2013), toxoplasmosis (Mikaeiloo, Ghaffarifar, Dalimi, Sharifi, & Hassan, 2016), and cancer, with fewer adverse effects than conventional chemotherapy (Alcântara et al., 2013).

In conclusion, our study showed that oral administration of free **artemether** had toxic effects on cardiomyocytes following a repeated-dose treatment regimen. Major effects involved NCX-dependent prolongation of the AP, explaining QTc prolongation and disrupted Ca^{2+} handling with a potential to trigger Ca^{2+}-dependent arrhythmias. However, these effects were totally prevented by nanoencapsulation of the drug in polymeric NCs. This strategy has the potential to improve therapeutic approaches to treat malaria, as well as other parasitic diseases, and to expand anti-tumour therapy, with **artemether**.

ACKNOWLEDGEMENTS

This work was supported by: a Bilateral Research Collaboration between Brazil (Capes: *Coordenação de Aperfeiçoamento do Pessoal de Nível* Superior, a Foundation within the *Ministry of Education*), and France (Cofecub: *Coopération universitaire et scientifique avec le Brésil*, funded by french *Ministère de l'Europe et des Affaires étrangères and Ministère de l'Enseignement supérieur, de la Recherche et de l'Innovation*) Me 768/13 and Me 978/20; CNPq (*Conselho Nacional de Desenvolvimento Científico e Tecnológico* of the *Brazilian federal government under the Ministry of Science*) with Researcher Grant 310463/2015-7; INCT (*National Institute of Science and Technology of Pharmaceutical Nanotechnology*–Nanofarma, Brazil.) 465687/2014-8; FAPEMIG (*Minas Gerais Research Foundation*, Brazil.) -Grants APQ-02576-18; and NANOBIOMG Network-Minas Gerais (RED-00007-14). The authors also would like to thank the Ministry of Health (*Programa Nacional de Controle da Malária-Brazil*) for their donation of Paluther® ampoules. ACM Souza is grateful for her scholarship grant from CAPES, CNPq, FAPEMIG (00432-13 and CDS-PPM-00481-13). We acknowledge the technical support provided by the *We-Met* Biochemistry platform (I2MC, Toulouse; info@we-met.fr) and the small animal imaging platform of Montpellier (IPAM; http://www.ipam.cnrs.fr) for echocardiography.

AUTHOR CONTRIBUTIONS

A.C.M.S., A.G.-G., J.D.S.C., L.T.O., V.C.F.M., and S.R. participated in research design. A.C.M.S., J.D.S.C., A.S.-M., L.T.O., A.L., P.S., C.F., and F.A. conducted the experiments. A.C.M.S., J.D.S.C., A.S.-M., L.T.O., F.A., and S.R. performed data analysis. A.C.M.S., A.G.-G., D.S.C., V.C.F.M., and S.R. wrote the manuscript.

CONFLICT OF INTEREST

The authors declare that there is no conflict of interest.

DECLARATION OF TRANSPARENCY AND SCIENTIFIC RIGOUR

This Declaration acknowledges that this paper adheres to the principles for transparent reporting and scientific rigour of preclinical research as stated in the *BJP* guidelines for Design and Analysis, Immunoblotting and Immunochemistry, and Animal Experimentation, and as recommended by funding agencies, publishers, and other organizations engaged with supporting research.

REFERENCES

Abreha, T., Hwang, J., Thriemer, K., Tadesse, Y., Girma, S., Melaku, Z., … Price, R. N. (2018). Comparison of artemether-lumefantrine and chloroquine with and without primaquine for the treatment of *Plasmodium vivax* infection in Ethiopia: A randomized controlled trial (PLoS medicine (2017) 14 5 (e1002299)). *PLoS Medicine*, *15*, e1002677. https://doi.org/10.1371/journal.pmed.1002677

Aditya, N. P., Patankar, S., Madhusudhan, B., Murthy, R. S. R., & Souto, E. B. (2010). Arthemeter-loaded lipid nanoparticles produced by modified thin-film hydration: Pharmacokinetics, toxicological and in vivo anti-malarial activity. *European Journal of Pharmaceutical Sciences*, *40*, 448–455.

Alcântara, D. D., Ribeiro, H. F., Cardoso, P. C., Araújo, T. M., Burbano, R. R., Guimarães, A. C., … de Oliveira Bahia, M. (2013). In vitro evaluation of the cytotoxic and genotoxic effects of artemether, an antimalarial drug, in a gastric cancer cell line (PG100). *Journal of Applied Toxicology*, *33*, 151–156.

Alexander, S. P. H., Fabbro, D., Kelly, E., Mathie, A., Peters, J. A., Veale, E. L., … CGTP Collaborators. (2019). THE CONCISE GUIDE TO PHARMACOLOGY 2019/20: Enzymes. *British Journal of Pharmacology*, *176*, S297–S396. https://doi.org/10.1111/bph.14752

Alexander, S. P. H., Kelly, E., Mathie, A., Peters, J. A., Veale, E. L., Armstrong, J. F., … CGTP Collaborators. (2019). THE CONCISE GUIDE TO PHARMACOLOGY 2019/20: Transporters. *British Journal of Pharmacology*, *176*, S397–S493. https://doi.org/10.1111/bph.14753

Alexander, S. P. H., Mathie, A., Peters, J. A., Veale, E. L., Striessnig, J., Kelly, E., … CGTP Collaborators. (2019). THE CONCISE GUIDE TO PHARMACOLOGY 2019/20: Ion channels. *British Journal of Pharmacology*, *176*, S142–S228. https://doi.org/10.1111/bph.14749

Anderson, M. E. (2015). Oxidant stress promotes disease by activating CaMKII. *Journal of Molecular and Cellular Cardiology*, *89*, 160–167.

Attili-Qadri, S., Karra, N., Nemirovski, A., Schwob, O., Talmon, Y., Nassar, T., & Benita, S. (2013). Oral delivery system prolongs blood circulation of docetaxel nanocapsules via lymphatic absorption. *Proceedings of the National Academy of Sciences of the United States of America*, *110*, 17498–17503.

Belardinelli, L., Shryock, J. C., & Fraser, H. (2006). Inhibition of the late sodium current as a potential cardioprotective principle: Effects of the late sodium current inhibitor ranolazine. *Heart Br. Card. Soc.*, *92*(Suppl 4), iv6–iv14.

Belew, S., Suleman, S., Mohammed, T., Mekonnen, Y., Duguma, M., Teshome, H., … de Spiegeleer, B. (2019). Quality of fixed dose artemether/lumefantrine products in Jimma Zone, Ethiopia. *Malaria Journal*, *18*, 236. https://doi.org/10.1186/s12936-019-2872-1

Bourgonje, V. J. A., Vos, M. A., Ozdemir, S., Doisne, N., Acsai, K., Varro, A., … Antoons, G. (2013). Combined Na^+/Ca^{2+} exchanger and L-type calcium channel block as a potential strategy to suppress arrhythmias and maintain ventricular function. *Circulation. Arrhythmia and Electrophysiology*, *6*, 371–379. https://doi.org/10.1161/CIRCEP.113.000322

Branquinho, R. T., Pound-Lana, G., Marques Milagre, M., Saúde-Guimarães, D. A., Vilela, J. M. C., Andrade, M. S., … Mosqueira, V. C. (2017). Increased body exposure to new anti-trypanosomal through nanoencapsulation. *Scientific Reports*, *7*, 1–12.

Branquinho, R. T., Roy, J., Farah, C., Garcia, G. M., Aimond, F., Le Guennec, J.-Y., … Richard, S. (2017). Biodegradable polymeric nanocapsules prevent cardiotoxicity of anti-trypanosomal lychnopholide. *Scientific Reports*, *7*, 44998. https://doi.org/10.1038/srep44998

Brossi, A., Venugopalan, B., Dominguez Gerpe, L., Yeh, H. J. C., Flippen-Anderson, J. L., Buchs, P., … Peters, W. (1988). Arteether, a new antimalarial drug: Synthesis and antimalarial properties. *Journal of Medicinal Chemistry*, *31*, 645–650. https://doi.org/10.1021/jm00398a026

Burgert, L., Rottmann, M., Wittlin, S., Gobeau, N., Krause, A., Dingemanse, J., … Penny, M. A. (2020). Ensemble modeling highlights importance of understanding parasite-host behavior in preclinical antimalarial drug development. *Scientific Reports*, *10*, 4410. https://doi.org/10.1038/s41598-020-61304-8

da Cesar, C. I., & Pianetti, G. A. (2009). Quantitation of artemether in pharmaceutical raw material and injections by high performance liquid chromatography. *Brazilian Journal of Pharmaceutical Sciences*, *45*, 737–742.

Chan, A., Isbister, G. K., Kirkpatrick, C. M. J., & Dufful, S. B. (2007). Drug-induced QT prolongation and torsades de pointes: Evaluation of a QT nomogram. *QJM: An International Journal of Medicine*, *100*, 609–615.

Chaurasia, M., Pawar, V. K., Jaiswal, A. K., Dube, A., Paliwal, S. K., & Chourasia, M. K. (2015). Chondroitin nanocapsules enhanced doxorubicin induced apoptosis against leishmaniasis via Th1 immune response. *International Journal of Biological Macromolecules*, *79*, 27–36.

Chimanuka, B., Gabriëls, M., Detaevernier, M. R., & Plaizier-Vercammen, J. A. (2002). Preparation of B-artemether liposomes, their HPLC-UV evaluation and relevance for clearing recrudescent parasitaemia in *Plasmodium chabaudi* malaria-infected mice. *Journal of Pharmaceutical and Biomedical Analysis*, *28*, 13–22.

Cumming, J. N., Ploypradith, P., & Posner, G. H. (1997). Antimalarial activity of artemisinin (qinghaosu) and related trioxanes: Mechanism(s) of action. *Advances in pharmacology San Diego Calif*, *37*, 253–297.

Curtis, M. J., Alexander, S., Cirino, G., Docherty, J. R., George, C. H., Giembycz, M. A., … Ahluwalia, A. (2018). Experimental design and analysis and their reporting II: Updated and simplified guidance for authors and peer reviewers. *British Journal of Pharmacology*, *175*, 987–993. https://doi.org/10.1111/bph.14153

Darpo, B., Karnad, D. R., Badilini, F., Florian, J., Garnett, C. E., Kothari, S., … Sarapa, N. (2014). Are women more susceptible than men to drug-induced QT prolongation? Concentration-QTc modelling in a phase 1 study with oral rac-sotalol. *British Journal of Clinical Pharmacology*, *77*, 522–531. https://doi.org/10.1111/bcp.12201

De Mello, C. G. C., Branquinho, R. T., Oliveira, M. T., Milagre, M. M., Saúde-Guimarães, D. A., Mosqueira, V. C. F., & de Lana, M. (2016). Efficacy of lychnopholide polymeric nanocapsules after oral and intravenous administration in murine experimental Chagas disease. *Antimicrobial Agents and Chemotherapy*, *60*, 5215–5222. https://doi.org/10.1128/AAC.00178-16

Denniss, A., Dulhunty, A. F., & Beard, N. A. (2018). Ryanodine receptor Ca^{2+} release channel post-translational modification: Central player in cardiac and skeletal muscle disease. *The International Journal of Biochemistry & Cell Biology*, *101*, 49–53.

El-Beshbishi, S. N., Taman, A., El-Malky, M., Azab, M. S., El-Hawary, A. K., & El-Tantawy, D. A. (2013). In vivo effect of single oral dose of artemether against early juvenile stages of *Schistosoma mansoni* Egyptian strain. *Experimental Parasitology*, *135*, 240–245.

Falade, C. O., Ogunkunle, O. O., Dada-Adegbola, H. O., Falade, A. G., de Palacios, P. I., Hunt, P., … Salako, L. A. (2008). Evaluation of the efficacy and safety of artemether-lumefantrine in the treatment of acute uncomplicated *Plasmodium falciparum* malaria in Nigerian infants and children. *Malaria Journal*, *7*, 246. https://doi.org/10.1186/1475-2875-7-246

Fessi, H., Puisieux, F., Devissaguet, J. P., Ammoury, N., & Benita, S. (1989). Nanocapsule formation by interfacial polymer deposition following solvent displacement. *International Journal of Pharmaceutics*, *55*, 1–4.

Funck-Brentano, C., Ouologuem, N., Duparc, S., Felices, M., Sirima, S. B., Sagara, I., … Voiriot, P. (2019). Evaluation of the effects on the QT-interval of 4 artemisinin-based combination therapies with a correction-free and heart rate-free method. *Scientific Reports*, *9*, 883. https://doi.org/10.1038/s41598-018-37113-5

Goldhaber, J. I. (1996). Free radicals enhance Na^+/Ca^{2+} exchange in ventricular myocytes. *The American Journal of Physiology*, *271*, H823–H833.

Grace, A. A., & Camm, A. J. (1998). Quinidine. *The New England Journal of Medicine*, *338*, 35–45.

Gu, Y. X., Cui, Y. F., Wu, B. A., Shi, X. C., & Teng, X. H. (1989). Effects of artemether on peripheral T, B, T mu and T gamma lymphocytes in beagle dog. *Journal of Traditional Chinese Medicine*, *9*, 215–219.

Haas, S. E., Bettoni, C. C., de Oliveira, L. K., Guterres, S. S., & Dalla Costa, T. (2009). Nanoencapsulation increases quinine antimalarial efficacy against *Plasmodium berghei* in vivo. *International Journal of Antimicrobial Agents*, *34*, 156–161.

Hagemann, D., & Xiao, R.-P. (2002). Dual site phospholamban phosphorylation and its physiological relevance in the heart. *Trends in Cardiovascular Medicine*, *12*, 51–56.

Hara, Y., Yamawaki, H., Shimada, M., Okada, K., Tanai, T., Ichikawa, D., … Kizaki, K. (2007). Anticholinergic effects of artemisinin, an antimalarial drug, in isolated guinea pig heart preparations. *Journal of Veterinary Medical Science*, *69*, 697–702. https://doi.org/10.1292/jvms.69.697

Haverkamp, W., Breithardt, G., Camm, J. A., & Janse, M. J. (2000). The potential for QT prolongation and proarrhythmia by non-antiarrhythmic drugs: Clinical and regulatory implications. *European Heart Journal*, *47*, 219–233.

Hernandez-Valladares, M., Rihet, P., & Iraqi, F. A. (2014). Host susceptibility to malaria in human and mice: Compatible approaches to identify potential resistant genes. *Physiological Genomics*, *46*, 1–16.

Isbister, G. K., & Page, C. B. (2013). Drug induced QT prolongation: The measurement and assessment of the QT interval in clinical practice. *British Journal of Clinical Pharmacology*, *76*, 48–57.

Kavishe, R. A., Koenderink, J. B., & Alifrangis, M. (2017). Oxidative stress in malaria and artemisinin combination therapy: Pros and Cons. *The FEBS Journal*, *284*, 2579–2591.

Kilkenny, C., Browne, W. J., Cuthill, I. C., Emerson, M., & Altman, D. G. (2010). Improving bioscience research reporting: The ARRIVE guidelines for reporting animal research. *Journal of Pharmacology and Pharmacotherapeutics*, *1*, 94–99.

Kurup, S. P., Butler, N. S., & Harty, J. T. (2019). T cell-mediated immunity to malaria. *Nature Reviews. Immunology*, *19*, 457–471.

Kuster, G. M., Lancel, S., Zhang, J., Communal, C., Trucillo, M. P., Lim, C. C., … Colucci, W. S. (2010). Redox-mediated reciprocal regulation of SERCA and Na^+-Ca^{2+} exchanger contributes to sarcoplasmic reticulum Ca^{2+} depletion in cardiac myocytes. *Free Radical Biology & Medicine*, *48*, 1182–1187. https://doi.org/10.1016/j.freeradbiomed.2010.01.038

Laxmi, M., Bhardwaj, A., Mehta, S., & Mehta, A. (2015). Development and characterization of nanoemulsion as carrier for the enhancement of bioavailability of artemether. *Artificial Cells, Nanomedicine, and Biotechnology*, *43*, 334–344.

Legrand, P., Barratt, G., Mosqueira, V., Fessi, H., & Devissaguet, J. (1999). Polimeric nanocapsules as drug delivery systems: A review. *STP Pharma Sci.*, *9*, 411–418.

Lehane, A. M., McDevitt, C. A., Kirk, K., & Fidock, D. A. (2012). Degrees of chloroquine resistance in Plasmodium—Is the redox system involved? *International Journal for Parasitology: Drugs and Drug Resistance*, *2*, 47–57.

Leite, E. A., Grabe-Guimarães, A., Guimarães, H. N., Machado-Coelho, G. L. L., Barratt, G., & Mosqueira, V. C. F. (2007). Cardiotoxicity reduction induced by halofantrine entrapped in nanocapsule devices. *Life Sciences*, *80*, 1327–1334.

Mikaeiloo, H., Ghaffarifar, F., Dalimi, A., Sharifi, Z., & Hassan, Z. M. (2016). Apoptotic activity and anti-Toxoplasma effects of artemether on the tachyzoites and experimental infected Vero and J774 cell lines by *Toxoplasma gondii*. *Indian Journal of Pharmacology*, *48*, 179–185.

Minamisawa, S., Hoshijima, M., Chu, G., Ward, C. A., Frank, K., Gu, Y., … Chien, K. R. (1999). Chronic phospholamban-sarcoplasmic reticulum calcium ATPase interaction is the critical calcium cycling defect in dilated cardiomyopathy. *Cell*, *99*, 313–322. https://doi.org/10.1016/S0092-8674(00)81662-1

Mortazavi Dehkordi, N., Ghaffarifar, F., Mohammad Hassan, Z., & Esavand Heydari, F. (2013). In vitro and in vivo studies of anti leishmanial effect of artemether on *Leishmania infantum*. *Jundishapur Journal of Microbiology*, *6*, 1–6.

Mosqueira, V. C. F., Loiseau, P. M., Legrand, P., Devissaguet, J., Bories, C., & Barratt, G. (2004). Efficacy and pharmacokinetics of intravenous nanocapsule formulations of halofantrine in *Plasmodium berghei*-infected mice. *Antimicrobial Agents and Chemotherapy*, *48*, 1222–1228.

Niggli, E., Ullrich, N. D., Gutierrez, D., Kyrychenko, S., Poláková, E., & Shirokova, N. (2013). Posttranslational modifications of cardiac ryanodine receptors: Ca^{2+} signaling and EC-coupling. *Biochimica et Biophysica Acta*, *1833*, 866–875.

Oguche, S., Okafor, H. U., Watila, I., Meremikwu, M., Agomo, P., Ogala, W., … Sowunmi, A. (2014). Efficacy of artemisinin-based combination treatments of uncomplicated falciparum malaria in under-five-year-old Nigerian children. *The American Journal of Tropical Medicine and Hygiene*, *91*, 925–935. https://doi.org/10.4269/ajtmh.13-0248

Orta-Salazar, G., Bouchard, R. A., Morales-Salgado, F., & Salinas-Stefanon, E. (2002). Inhibition of cardiac Na^+ current by primaquine. *British Journal of Pharmacology*, *135*, 751–763.

Ozdemir, S., Bito, V., Holemans, P., Vinet, L., Mercadier, J.-J., Varro, A., & Sipido, K. R. (2008). Pharmacological inhibition of Na/Ca exchange results in increased cellular Ca^{2+} load attributable to the predominance of forward mode block. *Circulation Research*, *102*, 1398–1405. https://doi.org/10.1161/CIRCRESAHA.108.173922

Pasquié, J.-L., & Richard, S. (2009). Prolongation in QT interval is not predictive of Ca^{2+}-dependent arrhythmias: Implications for drug safety. *Expert Opinion on Drug Safety*, *8*, 57–72.

Patel, K., Simpson, J. A., Batty, K. T., Zaloumis, S., & Kirkpatrick, C. M. (2015). Modelling the time course of antimalarial parasite killing: A tour of animal and human models, translation and challenges. *British Journal of Clinical Pharmacology*, *79*, 97–107.

Plewes, K., Leopold, S. J., Kingston, H. W. F., & Dondorp, A. M. (2019). Malaria: What's new in the management of malaria? *Infectious Disease Clinics of North America*, *33*, 39–60.

Price, R. N., Uhlemann, A. C., Brockman, A., McGready, R., Ashley, E., Phaipun, L., … Krishna, S. (2004). Mefloquine resistance in *Plasmodium falciparum* and increased pfmdr1 gene copy number. *Lancet*, *364*, 438–447. https://doi.org/10.1016/S0140-6736(04)16767-6

Reeves, J. P., Bailey, C. A., & Hale, C. C. (1986). Redox modification of sodium-calcium exchange activity in cardiac sarcolemmal vesicles. *The Journal of Biological Chemistry*, *261*, 4948–4955.

Salama, G., & Bett, G. C. L. (2014). Sex differences in the mechanisms underlying long QT syndrome. *American Journal of Physiology. Heart and Circulatory Physiology*, *307*, H640–H648.

Schiattarella, G. G., Altamirano, F., Tong, D., French, K. M., Villalobos, E., Kim, S. Y., … Hill, J. A. (2019). Nitrosative stress drives heart failure with preserved ejection fraction. *Nature*, *568*, 351–356. https://doi.org/10.1038/s41586-019-1100-z

Schillinger, W., Fiolet, J. W., Schlotthauer, K., & Hasenfuss, G. (2003). Relevance of Na^+–Ca^{2+} exchange in heart failure. *Cardiovascular Research*, *57*, 921–933.

Shah, S. M. H., Ullah, F., Khan, S., Shah, S. M. M., De Matas, M., Hussain, Z., … Isreb, M. (2016). Smart nanocrystals of artemether: Fabrication, characterization, and comparative in vitro and in vivo antimalarial evaluation. *Drug Design, Development and Therapy*, *10*, 3837–3850. https://doi.org/10.2147/DDDT.S114962

Shattock, M. J., Ottolia, M., Bers, D. M., Blaustein, M. P., Boguslavskyi, A., Bossuyt, J., … Xie, Z. J. (2015). Na^+/Ca^{2+} exchange and Na^+/K^+-ATPase in the heart. *The Journal of Physiology*, *593*, 1361–1382. https://doi.org/10.1113/jphysiol.2014.282319

Silamut, K., Newton, P. N., Teja-Isavadharm, P., Suputtamongkol, Y., Siriyanonda, D., Rasameesoraj, M., … White, N. J. (2003). Artemether bioavailability after oral or intramuscular administration in uncomplicated falciparum malaria. *Antimicrobial Agents and Chemotherapy*, *47*, 3795–3798. https://doi.org/10.1128/AAC.47.12.3795-3798.2003

Sneddon, L. U., Halsey, L. G., & Bury, N. R. (2017). Considering aspects of the 3Rs principles within experimental animal biology. *The Journal of Experimental Biology*, *220*, 3007–3016.

Sordet, F., Aumjaud, Y., Fessi, H., & Derouin, F. (1998). Assessment of the activity of atovaquone-loaded nanocapsules in the treatment of acute and chronic murine toxoplasmosis. *Parasite*, *5*, 223–229.

Souza, A. C. M., Mosqueira, V. C. F., Silveira, A. P. A., Antunes, L. R., Richard, S., Guimarães, H. N., & Grabe-Guimarães, A. (2018). Reduced cardiotoxicity and increased oral efficacy of artemether polymeric nanocapsules in *Plasmodium berghei*-infected mice. *Parasitology*, *145*, 1075–1083. https://doi.org/10.1017/S0031182017002207

Sowunmi, A., Akano, K., Ntadom, G., Ayede, A. I., Ibironke, F. O., Aderoyeje, T., … Happi, C. T. (2017). Therapeutic efficacy and effects of artemisinin-based combination treatments on uncomplicated *Plasmodium falciparum* malaria-associated anaemia in Nigerian children during seven years of adoption as first-line treatments. *Infectious Diseases of Poverty*, *6*, 36. https://doi.org/10.1186/s40249-016-0217-7

Svoboda, M., Poprach, A., Dobes, S., Kiss, I., & Vyzula, R. (2012). Cardiac toxicity of targeted therapies used in the treatment for solid tumours: A review. *Cardiovascular Toxicology*, *12*, 191–207.

Tanaka, H., Nishimaru, K., Aikawa, T., Hirayama, W., Tanaka, Y., & Shigenobu, K. (2002). Effect of SEA0400, a novel inhibitor of sodium-calcium exchanger, on myocardial ionic currents. *British Journal of Pharmacology*, *135*, 1096–1100.

Terentyev, D., Györke, I., Belevych, A. E., Terentyeva, R., Sridhar, A., Nishijima, Y., … Carnes, C. A. (2008). Redox modification of ryanodine receptors contributes to sarcoplasmic reticulum Ca^{2+} leak in chronic

heart failure. *Circulation Research*, *103*, 1466–1472. https://doi.org/10.1161/CIRCRESAHA.108.184457

Uchinoumi, H., Yang, Y., Oda, T., Li, N., Alsina, K. M., Puglisi, J. L., … Bers, D. M. (2016). CaMKII-dependent phosphorylation of RyR2 promotes targetable pathological RyR2 conformational shift. *Journal of Molecular and Cellular Cardiology*, *98*, 62–72. https://doi.org/10.1016/j.yjmcc.2016.06.007

Undrovinas, A. I., Belardinelli, L., Undrovinas, N. A., & Sabbah, H. N. (2006). Ranolazine improves abnormal repolarization and contraction in left ventricular myocytes of dogs with heart failure by inhibiting late sodium current. *Journal of Cardiovascular Electrophysiology*, *17*(Suppl 1), S169–S177.

Venetucci, L. A., Trafford, A. W., O'Neill, S. C., & Eisner, D. A. (2007). Na/Ca exchange: Regulator of intracellular calcium and source of arrhythmias in the heart. *Annals of the New York Academy of Sciences*, *1099*, 315–325.

Vidal-Diniz, A. T. (2014). Artemeter nanocapsules of, physical-chemical characterization, cardiotoxicity, neurotoxicity and efficacy in experimental malaria. PhD Theses Fed. Univ. Ouro Preto Ouro Preto Braz.

de Vries, P. J., & Dien, T. K. (1996). Clinical pharmacology and therapeutic potential of artemisinin and its derivatives in the treatment of malaria. *Drugs*, *52*, 818–836.

Wagner, S., Rokita, A. G., Anderson, M. E., & Maier, L. S. (2013). Redox regulation of sodium and calcium handling. *Antioxidants & Redox Signaling*, *18*, 1063–1077.

White, N. J. (2007). Cardiotoxicity of antimalarial drugs. *The Lancet Infectious Diseases*, *7*, 549–558.

World Health Organization. (2018). World malaria report.

Xu, H., Barry, D. M., Li, H., Brunet, S., Guo, W., & Nerbonne, J. M. (1999). Attenuation of the slow component of delayed rectification, action potential prolongation, and triggered activity in mice expressing a dominant-negative Kv2 alpha subunit. *Circulation Research*, *85*, 623–633.

Yin, J. Y., Wang, H. M., Wang, Q. J., Dong, Y. S., Han, G., Guan, Y. B., … Jing, S. F. (2014). Subchronic toxicological study of two artemisinin derivatives in dogs. *PLoS ONE*, *9*, 1–8.